

**State mixing in collisions involving highly excited barium atoms**

M. Allegrini,\* E. Arimondo,† E. Menchi,† C. E. Burkhardt, M. Ciocca, W. P. Garver, S. Gozzini,\* and J. J. Leventhal

*Department of Physics, University of Missouri–Saint Louis, 8001 Natural Bridge Road, Saint Louis, Missouri 63121*

J. D. Kelley

*McDonnell Douglas Research Laboratories, P.O. Box 516, Saint Louis, Missouri 63166*

(Received 23 October 1987)

With the use of two-step laser excitation, it is shown that the state distributions of highly excited barium atoms are substantially altered by inelastic collisions with barium atoms. For “pure” Rydberg states the initially produced *ns* or *nd* eigenstates are rapidly mixed with nearly degenerate *n'l'* states. For initially produced states that may be viewed as admixtures of Rydberg and doubly excited independent-electron eigenstates, collisions convert the distribution to one with nearly pure, albeit state-mixed, Rydberg character. Broadening of the absorption profiles of the highly excited states is also observed. This effect results from quasistatic interaction between two highly excited atoms during the excitation. Beyond a critical excited-atom density, avalanche effects lead to an apparent narrowing of these profiles which subsequently broaden at still higher atom density.

**I. INTRODUCTION**

Over the past decade or more, many properties of Rydberg atoms have been studied<sup>1</sup> both theoretically and experimentally. While much of the experimental work has been performed using “one-electron” alkali-metal atoms, the two-electron alkaline-earth atoms<sup>2</sup> have also received considerable attention. These two-electron systems afford the opportunity to observe and analyze interactions between singly excited Rydberg series and doubly excited valence states. Most previous studies have been directed toward elucidation of the intrinsic properties of these atoms.<sup>3–5</sup> In contrast, the work reported here was initiated to study collisional effects on the Rydberg states of barium, a two-electron atom with high-lying energy levels readily accessible with available laser wavelengths.

It has been shown that the various states that result from a nominal *5d7d* electronic configuration of atomic barium serve as perturbing states that alter the regularity of the *nd* Rydberg series.<sup>2</sup> For principal quantum numbers *n* above 20, the only significant perturber<sup>6,7</sup> is the one designated *5d7d*<sup>1</sup>*D*<sub>2</sub> which perturbs the *J*=2 Rydberg levels in the vicinity of *n*=26. This is illustrated in the partial term diagram shown in Fig. 1. The perturbed states can be written as linear combinations of the independent-electron singlet and triplet Rydberg states and the perturber

$$|\Psi_n\rangle = \alpha_n |6snd\ ^1D_2\rangle + \beta_n |6snd\ ^3D_2\rangle + \gamma_n |5d7d\ ^1D_2\rangle. \tag{1}$$

The fractional contributions of the singlet Rydberg, triplet Rydberg, and perturber components to these states are given by  $|\alpha_n|^2$ ,  $|\beta_n|^2$ , and  $|\gamma_n|^2$ , respectively. A number of interesting properties of highly excited Ba atoms can be understood using this independent-electron basis set.<sup>6,7</sup> Table I lists the fractional population

coefficients for several states near the *5d7d* perturber, the energy region of interest in the present study. The fact that the eigenstates have varying relative Rydberg–valence-state compositions in the vicinity of the perturber has important consequences with respect to the effects of collisions on these states. In this paper we report and discuss data that illustrate some of these effects.

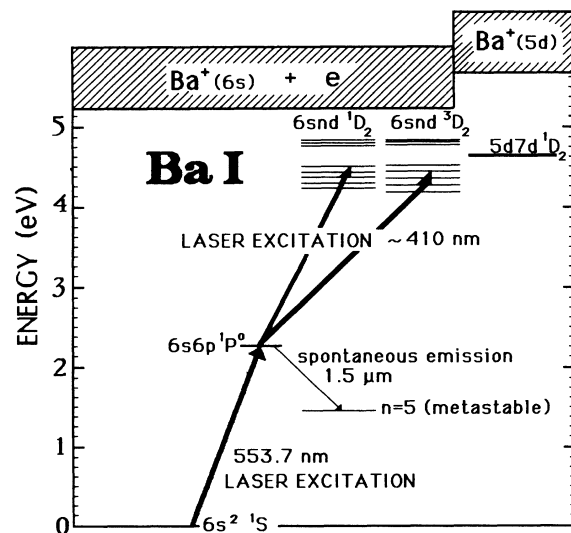


FIG. 1. Partial term diagram of Ba I illustrating the effects of the doubly excited *5d7d* state on the regularity of the singlet and triplet Rydberg series. The extent of level repulsion in these series is exaggerated for emphasis. This doubly excited state is also responsible for mixing of the singlet and triplet states. The two-step laser excitation used in these experiments is also illustrated.

TABLE I. Fractional Rydberg and perturber contribution to some  $J=2$  levels of Ba I.<sup>a</sup>

Nominal configuration	$^1D_2$			$^3D_2$		
	$ \alpha ^2$	$ \beta ^2$	$ \gamma ^2$	$ \alpha ^2$	$ \beta ^2$	$ \gamma ^2$
6s24d	0.78	0.20	0.013	0.20	0.79	0.0
6s25d	0.59	0.40	0.018	0.34	0.63	0.03
6s26d	0.59	0.28	0.125	0.28	0.71	0.13
5d7d			0.365			0.013
6s27d	0.76	0.05	0.189	0.08	0.91	0.009
6s28d	0.94	0.01	0.048	0.019	0.98	0.003
6s29d	0.98	0.002	0.019			

<sup>a</sup>Values taken from Ref. 6.

In a recent study<sup>8</sup> of processes that lead to ionization of Rydberg atoms we reported data that led to the conclusion that state changing, primarily  $nl \rightarrow nl'$ , of initially formed Na( $ns$ ) or Na( $nd$ ),  $18 \leq n \leq 35$ , was very rapid, with nearly geometric cross sections. Since such  $l$  mixing of Rydberg states is generally considered to be the result of collisions of the Rydberg electron and another atom or molecule, Na( $3s$ ) or Na( $3p$ ) in our earlier work, it is not surprising that the cross sections are comparable with the cross sectional area of the Rydberg atoms. The energy differences  $\Delta E$  between  $s$ ,  $p$ , and  $d$  states of both the  $n$  and adjacent manifolds of  $l$  states are considerably smaller than  $kT$  at these high values of  $n$ . Overlap of adjacent manifolds also occurs for the high-lying levels of barium; in fact, there are nearly four times as many levels as for sodium. It is, therefore, expected that collisional state changing will also be highly efficient. Indeed, we find this to be the case, but, not unexpectedly, only for the Rydberg component of the excited-state wavefunction. As a consequence, we find that a collection of barium atoms which has been laser excited to a perturbed level with a substantial  $5d7d$  fraction is rapidly converted, by collisions with other barium atoms, to a collection with a distribution over many nearly degenerate Rydberg states and essentially no  $5d7d$  character.

In addition to state changing we also report in this paper our observation that the excitation profiles of the highly excited states broaden dramatically with increasing excited atom density, an effect that we deduce to be the result of quasistatic interaction between highly excited atoms during the laser excitation.<sup>9</sup>

In addition to our studies of heavy-body collisional effects, we were also able to adjust experimental conditions so that we could observe the rapid and nearly complete conversion of Rydberg atoms to ions and electrons. This phenomenon, which is believed to be caused by an avalanche electron-impact ionization of Rydberg atoms, the "seed" electrons coming from, for example, photoionization by blackbody radiation, has been observed previously.<sup>10-12</sup> When the excited atom density is in excess of some threshold value,  $\sim 10^{14} \text{ cm}^{-3}$  under our experimental conditions, striking effects such as narrowing of absorption profiles and the absence of an allowed transition were observed.

## II. EXPERIMENTAL

The experiments were performed using a new apparatus, shown schematically in Fig. 2, employing a well-collimated beam of barium atoms and two grazing incidence dye lasers pumped by a single Nd:YAG laser. The collinear laser beams, one green and the other blue, intersected the atomic beam producing highly excited barium atoms, Ba<sup>\*\*</sup>, in two steps as illustrated in Fig. 1. Both laser beams were passed through the same linear polarizer before intersecting the Ba beam. The excitation region was electronically shielded to ensure field-free absorption. We observed that fields as low as  $\sim 1 \text{ V/cm}$  produced Stark mixing.

The atom density  $N$  in the beam was varied over the approximate range  $10^8 - 10^{13}$  as estimated from the oven temperature and vapor-pressure curves. We therefore consider the uncertainty in  $N$  to be roughly an order of magnitude; however, we were able to determine the ratios of different atom densities at which we worked with considerably higher precision. This was accomplished by detecting the Ba<sup>+</sup> resulting from two-step photoionization. With the green laser beam adjusted to saturate the  $6s^2 \ ^1S \rightarrow 6p \ ^1P$  resonance transition, the frequency-tripled output of the Nd:YAG laser was used to photoionize the Ba( $6p \ ^1P$ ). The ratio of the Ba<sup>+</sup> signal to the third harmonic power is proportional to the atom density, providing reliable ratios of atom densities at which various experiments were performed. The difficulty in determining the absolute value of  $N$  did, however, hamper our ability to accurately determine reaction cross sections.

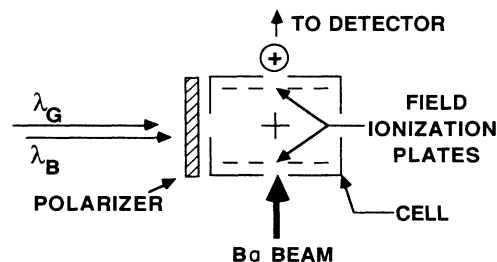


FIG. 2. Schematic diagram of the apparatus.

Two methods for detecting highly excited atoms were employed. At relatively low  $N$ ,  $\sim 10^8$ – $10^{10}$   $\text{cm}^{-3}$ , field ionization with a preset delay time, 200 ns to 2  $\mu\text{s}$ , produced  $\text{Ba}^+$  which were then detected with a CuBe particle multiplier. At the higher densities field ionization could not be used because of electrical breakdown of the vapor. The Rydberg states of interest in these experiments are, however, photoionized by room-temperature blackbody radiation. The resulting  $\text{Ba}^+$ , which were extracted normal to the plane defined by the laser beams and the atomic beam, were detectable, allowing this method to be used over the entire range of atom densities. No other ions, such as  $\text{Ba}_2^+$ , were observed when a quadrupole mass filter was used; this filter was subsequently removed to increase sensitivity.

The output of the CuBe particle multiplier was amplified, measured, and stored in a Radio Shack TRS-80 Color Computer which was suitably modified for both apparatus control and data acquisition. Most of the data reported here were acquired with the green laser beam wavelength fixed to the 553.7-nm resonance transition while scanning the blue laser beam wavelength,  $\lambda_B$ , thus yielding spectra of  $\text{Ba}^+$  signal versus blue wavelength. Care was taken to ensure that the detection system did not saturate, a condition that causes nonlinear gain. In such cases the absorption profile can be instrumentally broadened, yielding misleading data. Furthermore, nonlinear gain can alter the ratios of peak heights, giving for example, meaningless ratios for  $s$ -to- $d$ -state production. To avoid these spurious effects each time  $N$  or the laser power was increased, the electronic detection system was checked for linearity. This procedure is essential when absorption profiles and peak height ratios are compared at different values of  $N$  or  $N^{**}$ , the excited-atom concentration. Nonlinear gain of the electronic system is also important in experiments in which the Rydberg population rapidly evolves to a plasma via the avalanche mechanism. In this case it was necessary to decrease the overall sensitivity by moving the ion detector about 25 cm further from the excitation region than its usual location immediately outside the cell.

The laser beam intensities were 5 and 2  $\text{kW}/\text{cm}^2$  (maximum), respectively, for the green and blue lasers. At these levels the green resonance transition was saturated, but the blue transition to the highly excited states was not. The intensity of the blue laser beam was reduced when necessary using neutral density filters. The bandwidth of the green laser beam was about  $0.8 \text{ cm}^{-1}$ . For most of the experiments the bandwidth of the blue laser beam was also  $0.8 \text{ cm}^{-1}$ ; however, for some experiments, particularly those requiring careful comparison of absorption profiles, the mirror in the dye laser was replaced by a reflection grating, decreasing the bandwidth to  $0.2 \text{ cm}^{-1}$ .

### III. RESULTS AND DISCUSSION

Using prompt (200 ns) field ionization we obtain information on the initial population of highly excited states. Figure 3 is a field ionization (FI) spectrum,  $\text{Ba}^+$  signal versus  $\lambda_B$ , covering the region from  $n=26$  to ionization.

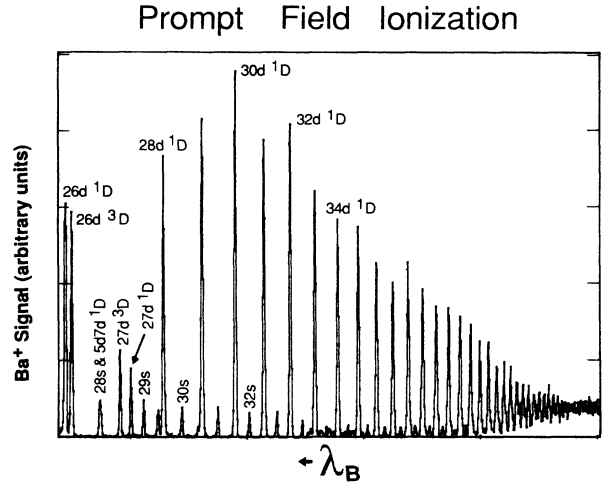


FIG. 3. Prompt field-ionization spectrum. The state designations are those commonly used (see Table I).

This spectrum illustrates salient features of highly excited Ba. Both  $6sns$  and  $6snd$  Rydberg states are formed, but perturbation of the  $6snd$  Rydberg states by the  $5d7d$  valence state in the region near  $n=26$  leads to a “hole” or dip in the peak heights in the spectrum.<sup>4</sup> This occurs because these eigenstates are linear combinations of Rydberg and  $5d7d$  valence perturbing state as shown in Table I. The region of the hole in the prompt (200 nsec) spectrum shown in Fig. 3 is due to the combined effects of radiative excitation and spontaneous decay; in particular the lifetimes of the most perturbed states are comparable with the 200-ns delay of the “prompt” FI pulse.

Collisions involving Rydberg atoms are preempted by prompt FI. To investigate the effects of such collisions we can delay the FI pulse. Of course other processes will also affect a delayed spectrum, principally radiative decay to a low-lying level if the delay time is comparable with the excited-state lifetime. Nevertheless, we compare delayed FI spectra taken at two different values of the atom density  $N$ . Figure 4 shows two spectra, each taken with a 2- $\mu\text{s}$  delay of the FI pulse. The most striking difference is the prominent peak at the  $27d \ ^1D_2$  wavelength in the higher density spectrum, a peak that is absent at the lower density. The absence of this peak at the lower density is the result of spontaneous decay of this short-lived state,<sup>7,13</sup>  $\tau \approx 300$  ns, prior to application of the FI pulse. Note that this state is not the most perturbed, nor is it the shortest lived.<sup>7,13</sup> These distinctions go to the state designated  $5d7d \ ^1D_2$ , but, because the energy of this state is nearly coincident with that of the pure Rydberg  $28s$  state, the evolution of  $5d7d \ ^1D_2$  atoms cannot be traced using the  $0.8\text{-cm}^{-1}$  bandwidth blue laser beam.

Returning to the data of Fig. 4, we see that the 2- $\mu\text{s}$  delay is nearly seven times the  $27 \ ^1D_2$  lifetime so that only about 0.1% of the initially produced excited atoms remain when the field ionization pulse is applied. The occurrence of a peak at the  $27d \ ^1D_2$  wavelength at the higher density clearly shows that the lifetime has been

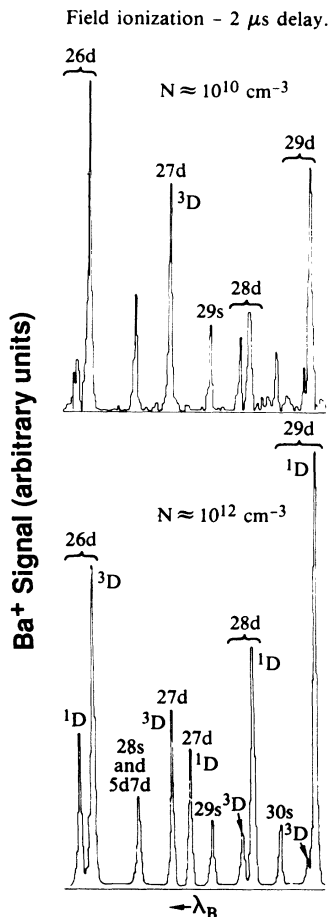


FIG. 4. Delayed (2- $\mu$ s) field-ionization spectra acquired at two different values of ground-state atom density  $N$ .

“lengthened,” presumably by heavy-body collisions. This terminology, though descriptive, is not precise. In actuality, heavy-body collisions cause state changing to states that are longer lived on the average.

There are other differences between the delayed FI spectra in Fig. 4. The singlet-to-triplet ratios for the 26d and 28d pairs of states change dramatically with  $N$ . In

both cases the shorter lived singlet states are more prominent in the higher density spectrum, again because of lifetime-lengthening collisions.

Although our experiments were not undertaken to measure excited-state lifetimes, we may estimate the lifetimes using our low-density prompt and delayed field ionization spectra. Comparison of these estimates with previously measured values may then be used as a reliability check of our apparatus. Table II lists some of our values along with those determined in two other experiments,<sup>7,13</sup> both of which were carefully designed for lifetime measurements. The table shows that our estimates are in reasonable agreement with both sets of data.

While delayed field ionization spectra taken at different atom densities can give information on some of the effects of heavy-body collisions, other effects cannot be traced using this method. Furthermore, electrical breakdown of the vapor prohibits use of FI at barium densities in excess of about  $10^{12}$   $\text{cm}^{-3}$ . Photoionization by blackbody radiation (BBPI) can, however, be employed at high densities, and can show effects which FI does not. BBPI is only useful when the ionization rate  $R_{nl}$  is high enough that ionization is not precluded by radiative decay.

For a given temperature  $T$ ,  $R_{nl}$  may be estimated from the relationship<sup>8,14</sup>

$$R_{nl} = \kappa(E_{nl})^2 / [\exp(E_{nl}/kT) - 1], \quad (2)$$

where  $E_{nl}$  is the ionization energy of the Rydberg state,  $k$  is the Boltzmann constant, and  $\kappa$  is a constant. Although an accurate value of  $R_{nl}$  depends on core effects, a useful estimate can be obtained from the values for sodium. Normalizing to the measured value<sup>8</sup> of  $R_{18d}$  for sodium at 500 K we obtain the series of curves shown in Fig. 5. Since the radiative rates of the states of interest vary, the relative peak heights in any spectrum acquired using BBPI to produce ions will depend on these lifetimes as well as  $R_{nl}$ . At low densities, effects due to heavy-body ionizing collisions are expected to be minimal. Since the charge collection time for each laser pulse is greater than either the radiative lifetimes or the reciprocals of  $R_{nl}$ , we may obtain the total ion signal per pulse  $Q$  by integration:

$$Q = \int_0^{\infty} RN^{**}(t) dt, \quad (3)$$

where  $N^{**}(t)$ , the excited-atom density, is given by

TABLE II. Comparison of measured lifetimes (in  $\mu$ s) of some  $J=2$  levels of Ba I.

Nominal electron configuration	Gallagher <i>et al.</i> <sup>a</sup>		Aymar <i>et al.</i> <sup>b</sup>		This work	
	<sup>3</sup> D <sub>2</sub>	<sup>1</sup> D <sub>2</sub>	<sup>3</sup> D <sub>2</sub>	<sup>1</sup> D <sub>2</sub>	<sup>3</sup> D <sub>2</sub>	<sup>1</sup> D <sub>2</sub>
6s25d	1.32	2.00	1.68	1.59		2.09
6s26d	2.00	0.35	1.91	0.49	2.00 <sup>c</sup>	0.66
6s27d	3.33	0.29	2.69	0.30	2.36	0.46
6s28d	2.57	0.89	3.23	0.90	2.55	0.91

<sup>a</sup>Reference 7.

<sup>b</sup>Reference 13.

<sup>c</sup>The value reported in Ref. 7 was assumed. The lifetimes calculated from our data are based on this assumed value for 6s26d <sup>3</sup>D<sub>2</sub> lifetime.

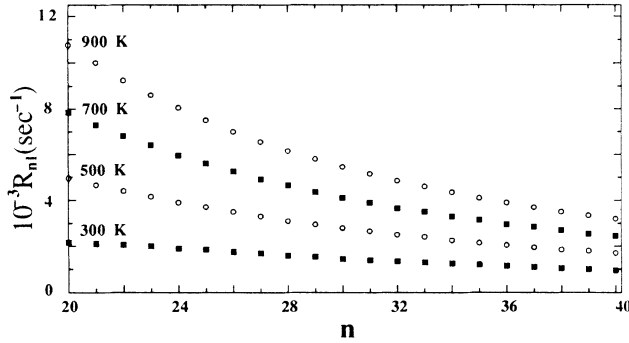


FIG. 5. Blackbody photoionization rate  $R_{nl}$  vs principal quantum number  $n$ , as calculated from Eq. (2). The absolute scale was normalized to the measured value of  $5700 \text{ s}^{-1}$  for  $\text{Na}(18d)$  at 500 K (Ref. 8).

$$\frac{dN^{**}(t)}{dt} = -AN^{**}(t) - RN^{**}(t). \quad (4)$$

In the above equation  $A$  is the spontaneous decay rate and, for simplicity, we have suppressed the  $nl$  subscripts with the understanding that these rates and densities apply to each state.

Integrating and designating  $N^{**}(t=0)$  by  $N_0^{**}$

$$Q = N_0^{**} R [1 / (A + R)]. \quad (5)$$

Since  $A \gg R$  and  $1/A = \tau$ , the radiative lifetime of the state

$$Q \simeq N_0^{**} R \tau. \quad (6)$$

Since  $R$  is slowly varying over the range  $25 \leq n \leq 30$ , Eq. (6) shows that the peaks corresponding to the longest-lived states will be enhanced when compared to the prompt FI spectrum.

We can examine the effects of heavy-body collisions on the lifetimes of the excited-state populations by comparing BBPI spectra acquired at different values of  $N$ . Figure 6 shows three such spectra. Also included is a synthetic spectrum based on Eq. (6); the relative values of  $N_0^{**}$  were taken from Fig. 3, BBPI rates from Eq. (2) and values of  $\tau$  from the literature.<sup>7,13</sup> This synthetic spectrum represents that expected for the collision-free case, i.e., when the atom density is low enough so that heavy-body collisions, either lifetime lengthening or ionizing, do not contribute significantly to the ion yield.

Despite some differences, the similarity of the synthetic spectrum to that acquired at the lowest  $N$  suggests that ionization at this value of  $N$  is due primarily to BBPI. An obvious difference between these two spectra is the relative heights of the peaks corresponding to the  $26d \ ^1D$  and  $26d \ ^3D$  states. It is interesting that if our estimated ratio of lifetimes (see Table II) were substituted, agreement between the two spectra would improve.

Comparison of the prompt FI spectrum in Fig. 3 with the collision-free BBPI spectrum in Fig. 6 shows that the pure Rydberg (unperturbed)  $d$ -state peaks are somewhat suppressed relative to the  $s$ -state peaks when BBPI is

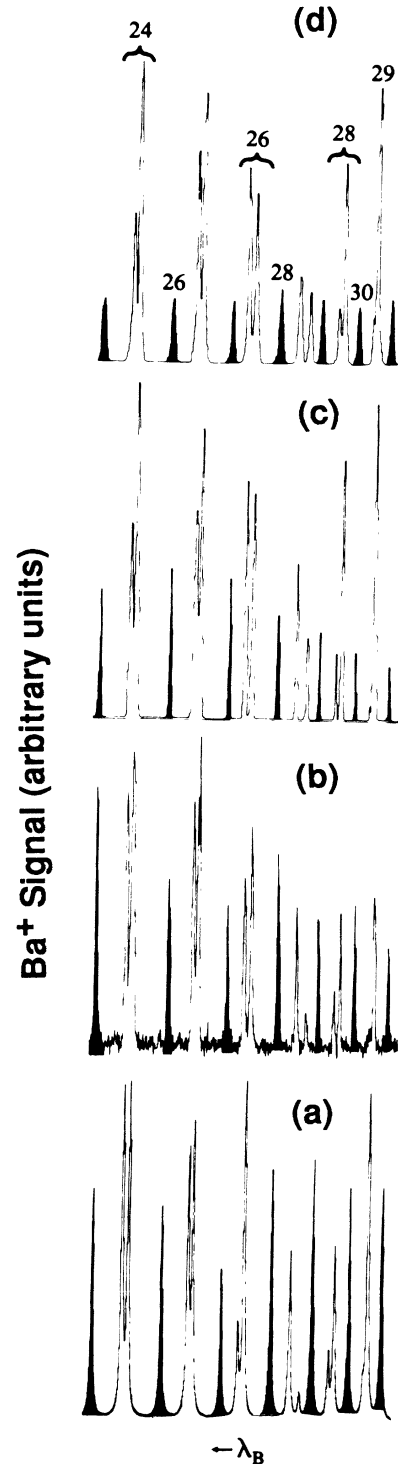


FIG. 6. (a) Synthetic spectrum calculated from Eq. (6). This spectrum represents that expected from blackbody photoionization (BBPI) in the absence of heavy-body collisions. (b)–(d) BBPI spectra taken at different values of  $N$ ; approximately  $10^{11}$ ,  $10^{12}$ , and  $10^{13} \text{ cm}^{-3}$ , respectively. The peaks for  $s$ -state excitations are shaded to facilitate comparison of the spectra; the unshaded peaks correspond to  $d$ -state excitations with the braces indicating singlet-triplet pairs. The blue laser beam bandwidth was  $0.8 \text{ cm}^{-1}$ . For more detailed identifications compare with Figs. 3 and 4.

used for detection. The major reason is that the radiative lifetimes of  $s$  states are longer than those of the pure  $d$  states of comparable principal quantum number.<sup>7,13,15</sup> Table III lists the lifetimes of some Ba I states pertinent to this point. As the density of ground-state barium atoms is increased, the peak heights of these shorter lived  $d$  states overtake those of the  $s$  states, the ratio tending toward that in the prompt FI spectrum, Fig. 3. In the high-density BBPI spectra, however, the lengthened lifetimes lead in the limit to  $Q = N_0^{**}$  because in this case  $A \ll R$ . Also, the peak corresponding to the highly perturbed, and hence short-lived,  $27d^1D$  state, while quite small in the collision-free spectrum, becomes increasingly prominent with increasing  $N$ . A similar effect is probably occurring for the most highly perturbed state, the one designated  $5d7d^1D$  with lifetime  $0.2 \mu\text{s}$ , but the near coincidence of energy, and therefore  $\lambda_B$ , with the  $28s$  state makes the effect unobservable with the  $0.8 \text{ cm}^{-1}$  bandwidth blue laser beam.

Although these data suggest that the state-changing collisions that cause lifetime lengthening are between the highly excited barium atoms  $\text{Ba}^{**}$  and ground state,  $6p^1P$  or  $5d^1D$  barium atoms (the last three of which we designate as Ba) additional experiments were undertaken to investigate the possible effects of  $\text{Ba}^{**}$ - $\text{Ba}^{**}$  collisions. First, we fixed the atom density  $N$  at a value comparable with that in Fig. 6(c) and varied the blue laser power density from maximum to 0.1 maximum and finally to 0.02 maximum, acquiring BBPI spectra at each laser power density. The three spectra, one of which is shown in Fig. 7(a), were identical, that is, the  $s$ -to- $d$  ratios were the same, as were the absorption profiles. Parenthetically we note that the narrow bandwidth blue laser beam ( $0.2 \text{ cm}^{-1}$ ) was used and therefore the  $28s$  and  $5d7d^1D_2$  states are resolved.

Since the *excited* atom density was varied by a factor of 50 in these constant  $N$  experiments, we infer that  $\text{Ba}^{**}$ - $\text{Ba}^{**}$  collisions do not produce lifetime lengthening. We next reduced  $N$  by a factor of 50 while keeping the laser power density of the blue beam at maximum. This effectively reduces both  $N^{**}$  and  $N$  by a factor of 50. The resulting BBPI spectrum, shown in Fig. 7(b), exhibits increased  $s$ -to- $d$  ratios, indicative of a tendency to-

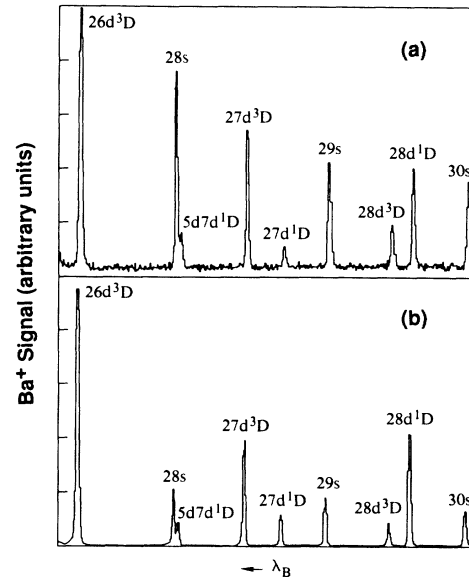


FIG. 7. (a) BBPI spectrum taken with  $N \sim 10^{12} \text{ cm}^{-3}$ . Three spectra taken at this value of  $N$ , each at different values of blue laser beam intensity, were identical (see text). (b) Same as (a) except  $N$  was lowered by a factor of 50. The higher ratio of  $s$ -to- $d$  peaks in this spectrum shows that collisions with ground-state (or low-lying excited-state) barium atoms are responsible for state changing, which effectively increases the lifetime of the excited-state population. The blue laser beam bandwidth was  $0.2 \text{ cm}^{-1}$ , narrower than that used to acquire the data displayed in Fig. 6 by a factor of 4, thus permitting partial resolution of the  $28s$  and  $5d7d^1D$  peaks.

ward collision-free conditions. This clearly establishes Ba as the major state-changing (lifetime-lengthening) collision partner.

The observed state mixing is consistent with an effective cross section comparable with the Rydberg geometric cross section, as has been observed in  $\text{Rb}^{**}$ - $\text{Rb}$  systems.<sup>16</sup> At  $n=25$ , the geometric cross section is  $3.4 \times 10^{-11} \text{ cm}^2$ , and the average Ba velocity at 1000 K is  $3.9 \times 10^4 \text{ cm s}^{-1}$ ; these values yield a state-mixing rate constant  $k_{\text{mix}} = 1.3 \times 10^{-6} \text{ cm}^3 \text{ s}^{-1}$ . Table III shows that the  $nd$  radiative lifetimes range from  $0.3$  to  $3 \mu\text{s}$ , while the  $ns$  lifetimes are appreciably longer. Both intuition and a simple rate-equation analysis lead to the conclusion that  $k_{\text{mix}}N$  values of  $10^5 \text{ s}^{-1}$  will alter the  $s$ -to- $d$  ratios from their collision-free values, and  $k_{\text{mix}}N \sim 10^6 \text{ s}^{-1}$  will produce substantial ratio changes. These first-order rate constants correspond to  $N$  values of  $10^{11}$  and  $10^{12} \text{ cm}^{-3}$ .

These data show that collisions with ground-state (or low-lying excited state) barium atoms do indeed "lengthen" the lifetimes of the excited atoms, especially  $d$  states. We suggest that these effects are due to  $nl$  mixing of the Rydberg components of the excited states, thus converting the initially produced excited states into states having substantial contributions from the statistically favored higher  $l$  states. For a one-electron atom, the radiative lifetime for a state with a specific value of  $l$  scales

TABLE III. Lifetimes in  $\mu\text{s}$  of some Ba I excited states that are conventionally designated  $6sns^1S_0$  and  $6snd^1,3D_2$ .

$n$	$^1S_0^a$	$^1D_2^b$	$^3D_2^b$
24	6.6	1.51	2.21
25	7.6	1.59	1.68
26	8.8	0.49	1.91
27	10.0	0.30	2.69
28	11.4	0.90	3.23
29	12.9	1.56	

<sup>a</sup>These are approximate values determined by extrapolating the experimental value for  $6s13s^1S_0$  using the established  $n^{*3}$  dependence of the lifetime;  $n^*$  is the effective quantum number (see Ref. 15).

<sup>b</sup>Reference 13.

as  $n^3$ , but the lifetimes of states with statistical distributions of  $l$  states scale as  $n^{4.5}$ . Thus as the density of ground-state barium atoms is increased, the lifetime of the excited-state population is increased, leading to a higher  $\text{Ba}^+$  yield from BBPI.

In addition to the effect on the excited-state lifetime, collisional state mixing also decreases the overall contribution of perturber character to the resulting distribution of excited states. If the perturber fraction remained roughly constant, no effect on the lifetime of the excited-state distribution would be observed since the short-lived valence component effectively determines the lifetimes. This is consistent with the expectation that the state-mixing cross section for Rydberg states is considerably larger than that for the much more localized valence states.

We may show that the perturber character of the admixture decreases by considering the wave function for an arbitrary excited atom in the distribution. We rewrite the eigenfunction of a laser excited  $d$  state in simplified form as

$$|\Psi_i\rangle = Z_{nd}^R |\psi_{nd}^R\rangle + Z^P |\psi^P\rangle, \quad (7)$$

where  $|\psi_{nd}^R\rangle$  and  $|\psi^P\rangle$  are Rydberg and perturber independent electron wave functions,  $|Z_{nd}^R|^2$  is  $(|\alpha_n|^2 + |\beta_n|^2)$  and  $|Z|^2$  is  $|\gamma_n|^2$ .

The effect of a time-dependent perturbation, a collision, on the initially produced state leads to a final-state wave function (for an arbitrary atom)

$$|\Psi_f\rangle = \sum_n \sum_l \bar{Z}_{nl}^R |\psi_{nl}^R\rangle + \bar{Z}^P |\psi^P\rangle. \quad (8)$$

This final-state wave function may also be written in terms of the *exact* energy eigenstates,  $|\phi_1\rangle$ ,  $|\phi_2\rangle \cdots |\phi_n\rangle$ , of the complete barium-atom Hamiltonian

$$|\Psi_f\rangle = A_1 |\phi_1\rangle + A_2 |\phi_2\rangle + \cdots. \quad (9)$$

Initially, however, the laser excitation produced a pure barium eigenstate, say,  $|\phi_1\rangle$ , so that  $|\Psi_i\rangle = |\phi_1\rangle$  and

$$|\Psi_f\rangle = A_1 (Z_{nd}^R |\psi_{nd}^R\rangle + Z^P |\psi^P\rangle) + A_2 |\phi_2\rangle + \cdots + A_n |\phi_n\rangle. \quad (10)$$

If it is assumed that only states within a few  $\text{cm}^{-1}$  of  $|\Psi_i\rangle$  are efficiently mixed by collisions, then  $|\phi_1\rangle$  is the only state in  $|\Psi_f\rangle$  that has any perturber character and  $\bar{Z}^P = A_1 Z^P < Z^P$ . For example, the eigenstate designated  $28d^1D_2$  (see Table I) is not collisionally mixed with  $26d^1D_2$  because of the large,  $20 \text{ cm}^{-1}$ , energy defect. Thus state mixing of the Rydberg component of the wavefunction leads to states with reduced perturber and increased, albeit mixed, Rydberg contribution.

Examination of Fig. 6 shows that as  $N$  is increased the absorption profiles broaden. In order to assign the source of this broadening we performed additional experiments using the narrow band ( $0.2 \text{ cm}^{-1}$ ) blue dye laser. States in the vicinity of  $n=40$  were prepared with  $N^{**} \sim 10^{11} \text{ cm}^{-3}$  and  $N \sim 10^{12} \text{ cm}^{-3}$ . The linewidths were measured, and the blue laser power was decreased progressively to

$0.1$  of the original level.  $N$  was kept constant. As the laser power was decreased, the linewidths decreased from about  $0.6 \text{ cm}^{-1}$  to about  $0.2 \text{ cm}^{-1}$ . Two typical spectra are shown in Fig. 8.

In a second set of experiments,  $N^{**}$  was kept constant, as measured by the BBPI signal, by increasing the blue power while decreasing  $N$ . The linewidths remained constant. Thus, the broadening is independent of  $N$ , but does depend on laser power for fixed  $N$ . These observations clearly show that the observed broadening is not caused by  $\text{Ba}^{**}\text{-Ba}$  collisions. The most plausible explanation for the broadening mechanism is that put forward by Raimond *et al.*<sup>9</sup> in their studies of highly excited Cs. They suggest that the dominant broadening mechanism is not collisional, but rather results from a quasistatic Rydberg-Rydberg interaction via the transition-dipole coupling matrix elements. This interaction splits the isolated Rydberg states into manifolds of closely spaced states, thus producing a broadened absorption profile. In fact, the slight red shading of these profiles in the upper spectrum of Fig. 8 may result from the attractive nature of the van der Waals interaction. Application of this model to our data leads to the conclusion that  $N^{**}$  values of  $2 \times 10^{11}$  and  $2 \times 10^{12} \text{ cm}^{-3}$  at  $n=40$  and  $n=25$ , respectively, will produce the  $0.6\text{-cm}^{-1}$  broadenings observed at the highest densities employed in making the linewidth observations reported here.

As the excited-atom density is increased to values higher than that employed to obtain the data shown in Figs. 3, 4, and 6, rapid evolution to a plasma occurs. This results in an ion signal so large that the detection system cannot be adjusted to avoid nonlinear and saturation effects. We therefore reduced the overall sensitivity by moving the particle multiplier about  $25 \text{ cm}$  away from the excitation region. Figure 9 shows  $\text{Ba}^+$  versus  $\lambda_B$

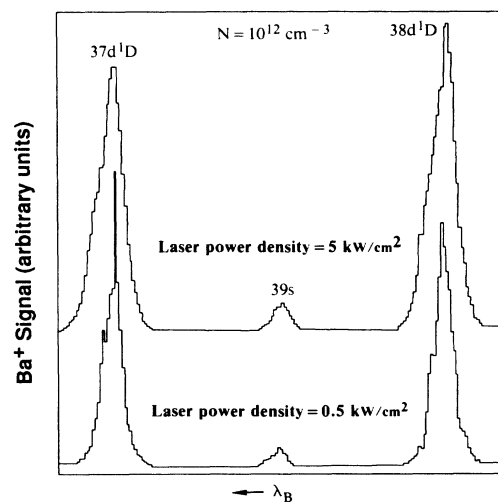


FIG. 8. BBPI spectra, both taken with  $N \sim 10^{12} \text{ cm}^{-3}$ . The power density of the blue laser beam used to acquire the lower spectrum was  $0.1$  that used to acquire the upper spectrum. These spectra demonstrate the dependence of the linewidths on  $N^{**}$ , the Rydberg atom density.

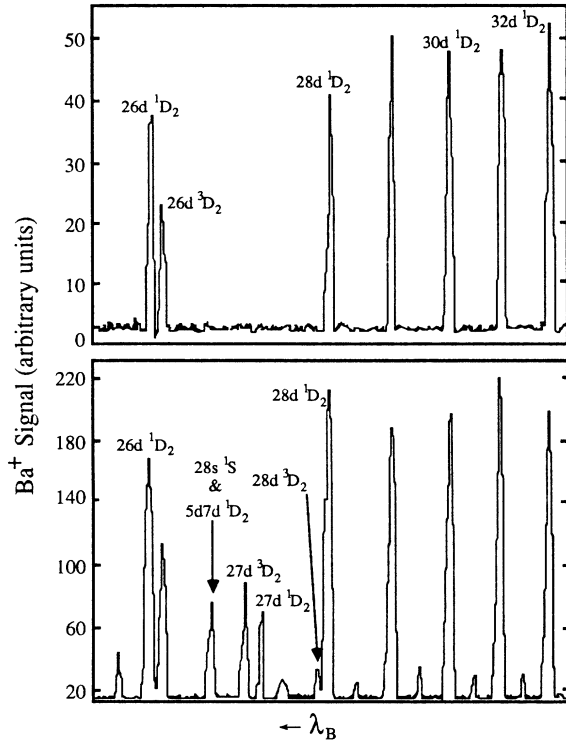


FIG. 9. Ion spectra acquired in the electron avalanche regime with  $N \sim 10^{14} \text{ cm}^{-3}$  (upper) and  $N \sim 5 \times 10^{14} \text{ cm}^{-3}$  (lower) using the reduced sensitivity setup.

spectra acquired at two different values of excited-atom density using this setup. The upper spectrum, the one acquired at the lower of the two densities, is noteworthy by the absence of any peaks in the hole or any peaks at wavelengths corresponding to  $s$  states. Furthermore, the  $d$ -state peaks are quite narrow in comparison to those in the lower (higher density) spectrum. In fact, we have observed that the excited-atom density can be reduced to a point at which the profiles are only one channel wide.

We interpret these observations as indicating a threshold value of  $N_0^{**}$  for evolution to a plasma, above which an avalanche of electron-impact ionization of the Rydberg atoms leads to complete ionization, an effect that has been observed previously.<sup>10-12</sup> The Rydberg component of the excited-atom density does not exceed this threshold value for the perturbed states and the  $s$  states under the conditions used to acquire the upper spectrum of Fig. 9. The reduced sensitivity prohibits detection of any ions resulting from either heavy-body collisions or BBPI for excitation of these states. Thus they are absent in the spectrum. Furthermore, as the profiles of the  $d$ -state peaks are scanned in  $\lambda_B$ ,  $N_0^{**}$  is below the threshold value in the wings and no ions are detected until line center is approached. Near line center a cascade of  $e$ - $\text{Ba}^{**}$  ionizing collisions leads to total ionization, and the signal is readily detectable with the reduced sensitivity. The seed electrons for this process can come from

heavy-body ionizing collisions or BBPI.

Because the lower spectrum in Fig. 9 was acquired with slightly higher excited-atom density, the threshold value of  $N_0^{**}$  is also reached for  $s$ -state peaks, as well as peaks in the hole, and even the  $28d \ ^3D$  state which was absent in the upper spectrum. Additionally, the  $d$ -state peaks in the lower spectrum are broader than the corresponding peaks in the upper spectrum, a result of the threshold now being exceeded further into the wings.

#### IV. SUMMARY

The work presented here shows that state changing in collisions of barium Rydberg atoms with ground-state or low-lying excited-state barium atoms is highly efficient. Because of this high efficiency, perturbed states, those that may be regarded as linear combinations of Rydberg- and valence-state-independent electron wave functions are rapidly converted by collisions to nearly pure, but  $nl$ -mixed, Rydberg states.

Broadened absorption profiles were also observed, but this effect is not the result of  $\text{Ba}^{**}$ - $\text{Ba}$  collisions. Rather, it results from a quasistatic  $\text{Ba}^{**}$ - $\text{Ba}^{**}$  dipole interaction during the excitation process.

Although state mixing is dominated by  $\text{Ba}^{**}$ - $\text{Ba}$  collisions, this does not mean that the dynamic part of the  $\text{Ba}^{**}$ - $\text{Ba}^{**}$  dipole interaction cannot cause state mixing, but only that this contribution is small. Similarly, the state-mixing collisions must contribute to line broadening, but to a negligible extent under the conditions of these experiments.

At excited-atom densities higher than those used to study state-changing collisions, initiation of the now well-known evolution of the excited-atom population toward a plasma was observed. This avalanche mechanism led to unusual effects in the spectra such as missing peaks and artificially narrowed absorption profiles.

Finally we note that the collisional alteration of the initial state-selected population by changing the Rydberg-to-perturber ratio may be used to contrast the reactivities of these two very different types of states. By changing the barium atom density in a laser-excited atomic beam we can change this ratio so that the effects of collision with another species will depend on the barium-atom density. Experiments of this type are planned.

#### ACKNOWLEDGMENTS

This work was supported by National Science Foundation (NSF) Grant Nos. PHY-8418075 and INT-8318024, U. S. Department of Energy (DOE) Grant No. DE-FG02-84ER1327, the McDonnell Douglas Independent Research and Development Programs, the University of Missouri Weldon Spring Fund, and the U. S. NSF and the Consiglio Nazionale delle Ricerche (CNR), Italy, Bilateral Research Programs No. 19931 (M.A. and S.G.) and No. 88.01280.02 (E. A. and E. M.) The authors wish to thank Professor T. F. Gallagher for useful discussions. One of us (S.G.) would like to thank the Council for International Exchange of Scholars for financial support.



\*Permanent address: Istituto di Fisica Atomica e Molecolare del Consiglio Nazionale delle Ricerche, Pisa, Italy.

†Permanent address: Dipartimento di Fisica dell' Università, Pisa, Italy.

<sup>1</sup>For a review see *Rydberg States of Atoms and Molecules*, edited by R. F. Stebbings and F. B. Dunning (Cambridge University Press, Cambridge, 1983).

<sup>2</sup>See, for example, M. Aymar, *Phys. Rep.* **110**, 163 (1984).

<sup>3</sup>A. Giusti-Suzor and U. Fano, *J. Phys. B* **17**, 4277 (1984), and references cited therein.

<sup>4</sup>W. Sandner, K. A. Safinya, and T. F. Gallagher, *Phys. Rev. A* **33**, 1008 (1986), and references cited therein.

<sup>5</sup>M. Aymar, P. Grafstrom, C. Levison, M. Lundberg, and S. Svanberg, *J. Phys. B* **15**, 877 (1982), and references cited therein.

<sup>6</sup>E. R. Eliel and W. Hogervorst, *J. Phys. B* **16**, 188 (1983).

<sup>7</sup>T. F. Gallagher, W. Sandner, and K. A. Safinya, *Phys. Rev. A* **23**, 2969 (1981).

<sup>8</sup>C. E. Burkhardt, R. L. Corey, W. P. Garver, J. J. Leventhal, M. Allegrini, and L. Moi, *Phys. Rev. A* **34**, 80 (1986).

<sup>9</sup>J. M. Raimond, G. Vitrant, and S. Haroche, *J. Phys. B* **14**, L655 (1981).

<sup>10</sup>G. Vitrant, J. M. Raimond, M. Gross, and S. Haroche, *J. Phys. B* **15**, L49 (1982).

<sup>11</sup>E. F. Worden, J. A. Paisner, and J. G. Conway, *Opt. Lett.* **3**, 156 (1978).

<sup>12</sup>C. E. Burkhardt, W. P. Garver, V. S. Kushawaha, and J. J. Leventhal, *Phys. Rev. A* **30**, 652 (1984).

<sup>13</sup>M. Aymar, R.-J. Chamean, C. Delsart, and J.-C. Keller, *J. Phys. B* **14**, 4489 (1981).

<sup>14</sup>W. P. Spencer, A. G. Vaidyanathan, D. Kleppner, and T. W. Ducas, *Phys. Rev. A* **26**, 1490 (1982).

<sup>15</sup>M. Aymar, P. Grafstrom, C. Levison, H. Lundberg, and S. Svanberg, *J. Phys. B* **15**, 877 (1982).

<sup>16</sup>M. Hugon, F. Gounand, and P. R. Fournier, *J. Phys. B* **13**, L109 (1980).